Ocean and Coastal Research

ORIGINAL ARTICLE

http://doi.org/10.1590/2675-2824072.23081
ISSN 2675-2824

The climatology and classification of coastal storms on the Southeastern coast of Rio de Janeiro State, Brazil

Leonardo Klumb-Oliveira[1]*

[1] Centro de Ciências Agrárias, Ambientais e Biológicas – Universidade Federal do Recôncavo da Bahia (Av. Ruy Barbosa, 710 – CEP 44380000 – Centro – Cruz das Almas – BA – Brazil).

* Corresponding author: leonardoklumb@ufrb.edu.br

ABSTRACT

The storm risks in coastal regions have drawn attention worldwide in recent decades. Understanding the characteristics and behavior of these events and their potential damage to coasts has become essential for decision-making and coastal management. This study aimed to identify and examine the climatology of coastal storms on the central coast of the state of Rio de Janeiro, proposing a classification and a coastal impact evaluation that applies Dolan and Davis' (1992) storm index. For this, 34 years of NOAA/NCEP/NCAR hindcast wave database were used (1979 - 2013). Secondarily, this study aimed to compare wave data at two locations (the south-orientated west and the east-northeast-orientated east coasts) to verify the influence of coastal orientation against storm events. This research found 231 storm events on the west coast and 44 on the east coast. While mean durations resembled each other (at around 27 hours), the east coast had a 9% lower mean storm wave height. The storm peak direction from the south predominated on the west coast (52%), whereas a south-southeast direction dominated the east coast (50%). Storm classification showed 3.4 and 9% of storms considered Extreme in the west and east, respectively. Extreme storms include those in September 1983, May 1997, May 2001, and April 2010. Coastal storms on the west and east represented 2.39 and 0.57% of all cyclones identified in the southwestern Atlantic. In shallow waters, the highest amount of energy dissipation occurred on the east coast, which is sheltered from storms from the south-southwest but is exposed to those from the south-southeast. Extreme and Severe events greatly impacted the coast, including beach and dune erosion, overwash, and property damage. However, even coastal storms considered Weak caused considerable coastal damage.

Keywords: Storm power index, Extratropical cyclones, Coastal orientation, Shallow water energy dissipation

INTRODUCTION

Surface waves are the primary energy source for coastal environments, especially in regions subject to microtidal regimes. Seasonal variations of wave energy are recurring on the coast when beaches adapt their morphology to the prevailing wave patterns (Shepard, 1950; Bruun, 1962). Eventually, meteorologically induced higher energy waves can trigger long-term beach erosion and severely damage coastal urban structures. These storm events can be defined as coastal storms (Harley, 2017), and they can cause prolonged high energy influx in the coastal environment, leading to cumulative damage. Damage recovery costs have totaled millions of dollars per storm worldwide (Mitchell, 1974).

Extratropical cyclones are one of the primary meteorological sources of energy from the wind to

Submitted: 30-May-2023
Approved: 18-May-2024

Associate Editor: Eduardo Siegle

the sea surface, resulting in high-energy sea states along its position and displacement. The Western South Atlantic Ocean is a well-known cyclogenetic region, especially southern Brazil, the southeastern coast of Argentina, and the southeastern coast of Uruguay (Gan and Rao, 1991; Reboita et al., 2010). Once generated, these cyclones tend to follow an east, southeast, or northeast trajectory over the Atlantic Ocean (Gan and Rao, 1991; Innocentini and Prado, 2003; Parise et al.,2009), with an average life cycle of 72 hours (Reboita et al., 2009) that may span up to 240 hours (Abreu et al., 2018). These cyclones frequently generate high-energy waves in deep water that propagate across the ocean and reach shallow areas of coastal regions (Rocha et al., 2004).

As the storm waves reach the coastal waters, their speed and wavelength decrease, and part of their energy is dissipated by bottom friction and depth-induced breaking. Non-dissipative forces such as wave refraction also occur, changing coastal storm wave behavior (Collings, 1970; Battjes and Groenendijk, 2000). Thus, coastline orientation, degree of exposure to storm waves, and inner shelf morphology play an essential role in predicting shoreline changes and coastal vulnerability (Dolan and Hayden, 1983).

The nearshore impact on natural and urban areas of coastal storms is featured in the literature on the southern and southeastern Brazilian coast. Beach erosion, foredune overwash, inundation, and destruction of local infrastructure were observed after coastal storms on the coast of Rio Grande do Sul (Parise et al., 2009; Barletta and Calliari, 2002), Santa Catarina (Rudorff et al., 2014), São Paulo (Sondermann et al., 2023), and Rio de Janeiro (Lins-de-Barros, 2005; Muehe, 2011; Muehe et al., 2015; Bulhões et al., 2016; Carvalho et al., 2020). Thus, understanding the dynamics and storm climatology is relevant for preventing and mitigating coastal natural threats.

Since the 1980s, several studies have examined coastal storms (especially on the North Atlantic coast), considering different variables such as wind speed, sea level, wave energy, storm duration, and coastal impacts (Allen, 1981; Dolan and Davis, 1992; Zhang et al., 2000; Ojeda et al., 2017; Kutupoglu et al., 2023). Regarding the South Atlantic, the availability of data measured in situ is scarce.

Paula et al. (2015) identified the lack of historical observational data on waves as the primary limitation for a better understanding of nearshore storm impacts. To address this issue, hindcast wave data have emerged as an alternative. These data enable climatological analysis by providing globally covered spatially and temporally gridded data over a long period. The possibility of reconstructing past climatological scenarios made the hindcast capable of being applied in the most diverse regions and with multiple application areas (Poli, 2011).

In the central coast of Rio de Janeiro State, Brazil, the coastline shifts its orientation at the municipalities of Arraial do Cabo and Cabo Frio (approximately at 22.99°S/41.99°W) and thus divides this part of the coast into two orientated shorelines: the western coast, approximately west-east (W-E) orientated, and the eastern coast, southwest-northeast (SW-NE) orientated, from the north of Cabo Frio to the Cape São Tomé. This study aims to identify and examine the climatology of coastal storms on the central coast of the state of Rio de Janeiro, evaluating coastal storms and their impacts on the coast. Additionally, it will compare the wave climatology of the two coastal sectors to understand the role of coastal orientation in natural storm protection.

METHODS

Study Area

The study area is located on the central coast of the state of Rio de Janeiro, Brazil. This study follows a regional approach on a scale of approximately 1:50.000. It covers the wave climate that extends from the continental shelf up to the limits of the shoreface, corresponding to the coastal zone of the municipalities between Saquarema and Arraial do Cabo, in the coastal segment here called the Western Coastal Sector (WCS), and between Cabo Frio and Cape São Tomé, in the so-called East Coastal Sector (ECS) (Figure 1).

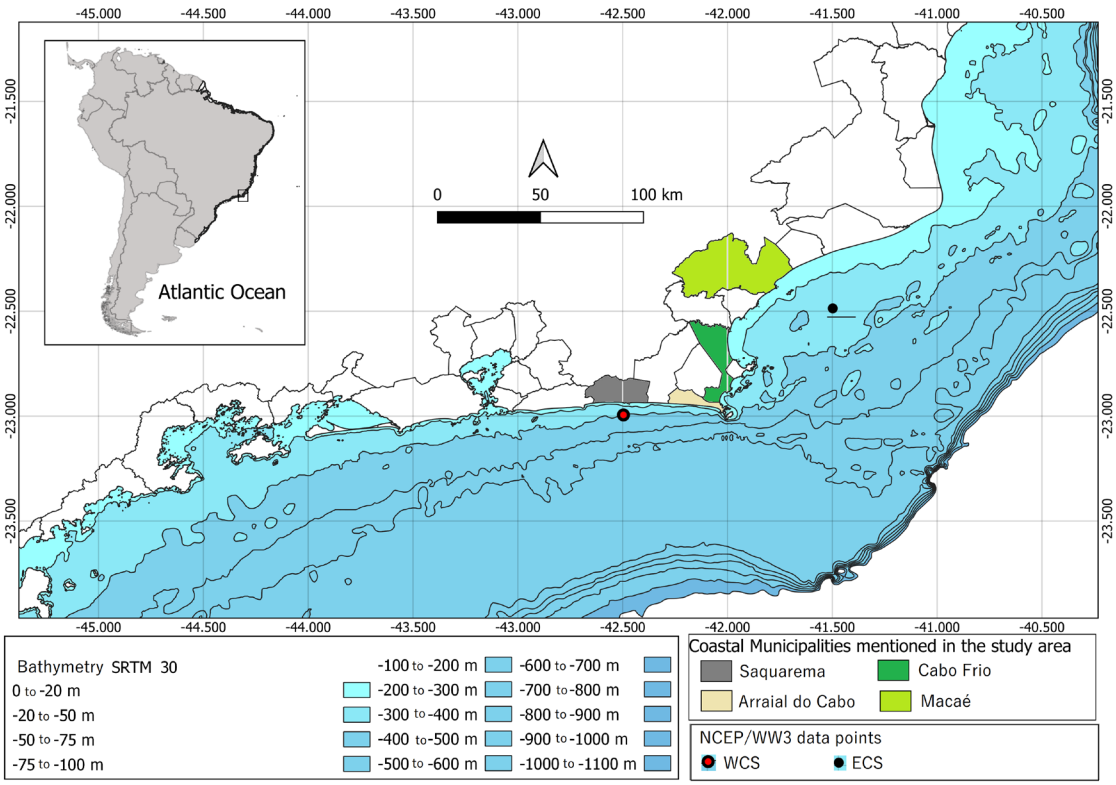

Figure 1. Map of the study area, showing the position of wave databases and the mentioned municipalities. Bathymetry data is available at https://geosgb.sgb.gov.br/downloads/.

According to Figueredo Jr. et al. (2016), the Campos Basin continental shelf has a maximum width of 120 km in its southern portion, between Cabo Frio and Macaé. The Santos Basin continental shelf, close to Cabo Frio, shows narrowing, reaching widths close to 75 km (Figueiredo et al.,2023).

The ECS coastal plain has features such as the cliffs of the Barreiras Formation, with exposed beach rocks and coral reefs. Its fluvial drainage contribution is significant, and the sedimentary inner shelf predominantly consists of coarse sand superimposed by a layer of very thin sand (Muehe and Valentini, 1998), with high levels of bioclasts (~50%) (Figueredo Jr. and Tessler, 2004). The Brazilian Hydrographic Navy Center bathymetric data compiled by Reis et al. (2013) indicated an average gradient of 0.1° in its inner shelf.

The WCS is characterized by double beach-barrier ridges that confine coastal lagoons in a typical lagoon-barrier (beach barrier) system named the strand plain of Massambaba. Its inner shelf is composed of coarse sand with a low presence of bioclasts (< 30%) and an average gradient of 0.5° (Figueredo Jr. and Tessler, 2004).

The wave climate of the coast of Rio de Janeiro State is predominantly influenced by large-scale meteorological systems, such as the South Atlantic Subtropical High (SASH), and extratropical lows (cyclones), as stated by Campos et al. (2013) and Parente et al. (201). SASH is responsible for the predominantly trade winds along the Brazilian coast, generating waves with northeastern, eastern, and eastern-southeastern peak directions (Dp). In the fall, winter, and early spring, extratropical cyclones become more frequent, resulting in higher energy wave formation and drawing nearer to the coastline from its South quadrants.

Storm climatology and classification

The climatology of the storm events was developed using a 34-year (1979-2013) wave data hindcast, available from the National Oceanic and Atmospheric Administration/National Centers for Environmental Prediction (NOAA/NCEP),

which was derived from the third-generation wind-wave model WAVEWATCH III® (Tolman, 2009), phase 1 and 2. The model was forced with winds from the NCEP-Climate Forecast System Reanalysis (CFSR) (Saha et al., 2010), hereafter called NCEP/WW3. These wave data were available eight times daily (00:00, 03:00, 06:00, 09:00, 12:00, 15:00, 18:00, and 21:00 UTC) at a global 0.5° × 0.5° Lat/Long-grid points. Overall, three variables were used to develop the storm climatology: Hs (Significant Height, meters), Tp (Peak period, seconds), and Dp (Peak Direction, degrees). In total, two grid points were chosen to represent different coastal orientations: WCS and ECS (Table 1, Figure 1)

Table 1. Grid points and their respective coordinates and mean depth

Grid Point	Coordinate	Mean Depth (m)	Coastal Orientation
WCS	23°S - 42.5°W	50	west-east
ECS	22.5°S - 41.5°W	45	southwest--northeast

Storm events were identified using two parameters: significant wave height (Hs) and time duration (td, measured in hours). An automated routine was used to find the starting date and time on the time series when the minimum Hs and td thresholds were identified, and it ended when the Hs value decreased below the threshold. The threshold values were chosen based on the average value of 5% of the largest waves in the database (Hs 5%), as suggested by Durán et al. (2016) and Earlie et al. (2018). A time duration value of 12 hours was selected as it represented the value of a semi-diurnal tidal cycle (You and Lord, 2008). In this study, a 5% Hs value represented three meters, considering the WCS dataset. For a fair comparison, this value was used to identify storm events at both wave data points. Therefore, this study considers a storm event as one with a Hs of at least three meters for at least 12 hours.

The storm classification was based on the Storm Power Index (SPI) proposed by Dolan and Davis (1992):

$$\int Hs^2 \star td \quad (1)$$

In which Sh (m) is the maximum wave height and td, the time of duration (hours) of the storm. The identified storm events were then grouped into five classes, according to the Jenks Natural Breaks Classification Method (Jenks, 1967). The method is widely used for several grouping purposes (Naiqiang and Guiyang, 2020). It aims to maximize the variance between classes as it seeks to reduce the variance within each class. This method was also used by Rangel-Buitrago and Anfuso (2011) for group coastal storm classes on the coast of Spain.

As suggested by Dolan and Davis (1992), from the smallest to the largest values of equation 1, the identified storms were classified into five storm classes: Class I (Weak), Class II (Moderate), Class III (Significant), Class IV (Severe), and Class V (Extreme). Each class represents progressively increasing coastal impact, according to the authors. Class Weak causes small beach erosion, with full and immediate recovery. Class Moderate shows modest beach erosion, but may damage local property. Class III provokes moderate beach and dune erosion and more extensive property damage. Class Severe shows severe beach erosion with rare recovery, dune erosion, overwash, and intense property damage. Class Extreme causes extreme beach erosion, long-term erosive trends, extreme dune erosion, overwash, and property damage on a regional scale.

The returning period was calculated in terms of annual maximum storm power, using the probability distribution analysis approach and extreme values following the Gumbel distribution.

Shallow water wave propagation

To propagate storm waves to shallow areas, the Mild Slope Parabolic Model for Monochromatic Wave Propagation (OLUCA-MC) was used. The OLUCA-MC is part of the Integral Model of Wave Propagation, Currents, and Morphodynamics in Beaches from IH Cantabria (IH CANTABRIA – MMA, 2017). The model solves the equations of refraction, diffraction, and energy dissipation by the finite difference method on a rectangular grid. As initial conditions, four storms in the Extreme and Severe Classes were chosen to represent

the most different peak directions, e.g., east-southeast, south-southeast, south, and south-southwest. This enabled the evaluation of the effect of refraction between the sectors of the coast. The mean significant height, peak period, and angle of direction associated with the chosen storm event were set.

For each propagation scenario, a specific mesh was created to adjust to different propagation angles. In all cases, wave dispersion was set up using the Stokes-Hedges non-linear model, using the turbulent boundary layer for dissipation and open lateral boundaries as boundary conditions.

Coastal Impacts

The assessment of coastal impacts was carried out by reviewing publications that described the effects of storms on both coastal sectors. The impacts observed in the literature were correlated with the classes of storms identified in this study and were then compared with the impacts predicted for each class, according to those observed by Dolan and Davis (1992). The assessed variables were based on the occurrence of beach erosion (which was divided into weak, moderate, or severe categories), dune erosion (including dune base escarpment and crest retreat), property damage (the destruction of rigid structures along the coast), and overwash (a flow of water and sediment over a coastal dune or beach crest).

RESULTS

NCEP/WW3 Hindcast data validation

Klumb-Oliveira et al. (2015) compared the Hs, Dp, and Tp of the same grid point (WCS) in this study with a stationary oceanographic buoy near the study area (22.99S; 42.18W, depth, 50 m). The authors found a Pearson's correlation of 0.79 for Hs, 0.53 for Dp, and 0.75 for Tp. Hs showed the highest hindcast overestimation: 0.47 m. For Dp, the hindcast data overestimated the buoy data by 0.16 s. Peak direction data showed a lower correlation due to the differences between local average conditions and peak directions. According to their results, the authors considered that validation authenticates the use of NCEP/WW3 hindcast data as a wave parameter for coastal studies in Rio de Janeiro. Furthermore, Carvalho et al. (2020) compared an NCEP/WW3 grid point at the west coast of Rio de Janeiro with a buoy anchored off the Rio de Janeiro coast. The authors found a 'moderate' to 'strong' correlation between field and hindcast data, which also validates the data for climatological analysis.

Storm climatology

Following the criteria above (Hs 3 m and Td 12 h), 231 storm events were identified in the WCS and 44 in the ECS, averaging 6.8 and 1.2 events yr^{-1}, respectively. In the WCS, mean Hs totaled 3.5 m± 0.35; mean Tp 12s±1.7; and mean Dp, 187±13. Peak direction predominantly stemmed from the south (52.6 %) and south-southwest (39%), with a lower frequency of waves coming from the south-southeast (7.2 %). The south and south-southwest directions also showed the highest waves (≥ 4 m), with the prevalence of wave height from three to four meters. The peak period from 8 to 10 s showed the lowest frequencies in all directions. South and south-southwest showed a similar distribution of periods from 10 to 14s. Periods above 14s predominantly stemmed from the south (Figure 2).

The ECS showed mean Hs values of 3.3 m± 0.28, mean Tp of 12.5 s± 2.2, and mean Dp of 161± 15. ECS storms predominantly came from the south-southeast (50 %) and south (36 %), with a lower frequency coming from the southeast (9 %) and east-southeast (4 %). Although with lower frequency, the east-southeast direction showed high waves above 4 m (Figure 2). A comparison between the two grid points shows similar values of mean significant wave height and peak period that considerably differ in peak direction. A remarkable observation is the absence of storms coming from the east-southeast at the WCS and the absence of storm waves from the south-southwest at ECS.

The mean storm duration for both coastal sectors was similar to each other, with WCS and ECS experiencing durations of 27.8 and 27.0 h that ranged from 12 h to 90 h, respectively. However, regarding storm direction, WCS showed longer storms from the south and south-southwest, whereas ECS, longer storms from the south-southeast and east-southeast. In both coastal

sectors, the prevailing time duration ranged from 12 to 27 hours. WCS and ECS showed the same value regarding the longest storm, 90 h, although in different episodes: in August 2011 (predominantly from the south) and September 1983 (predominantly from the east-southeast), respectively.

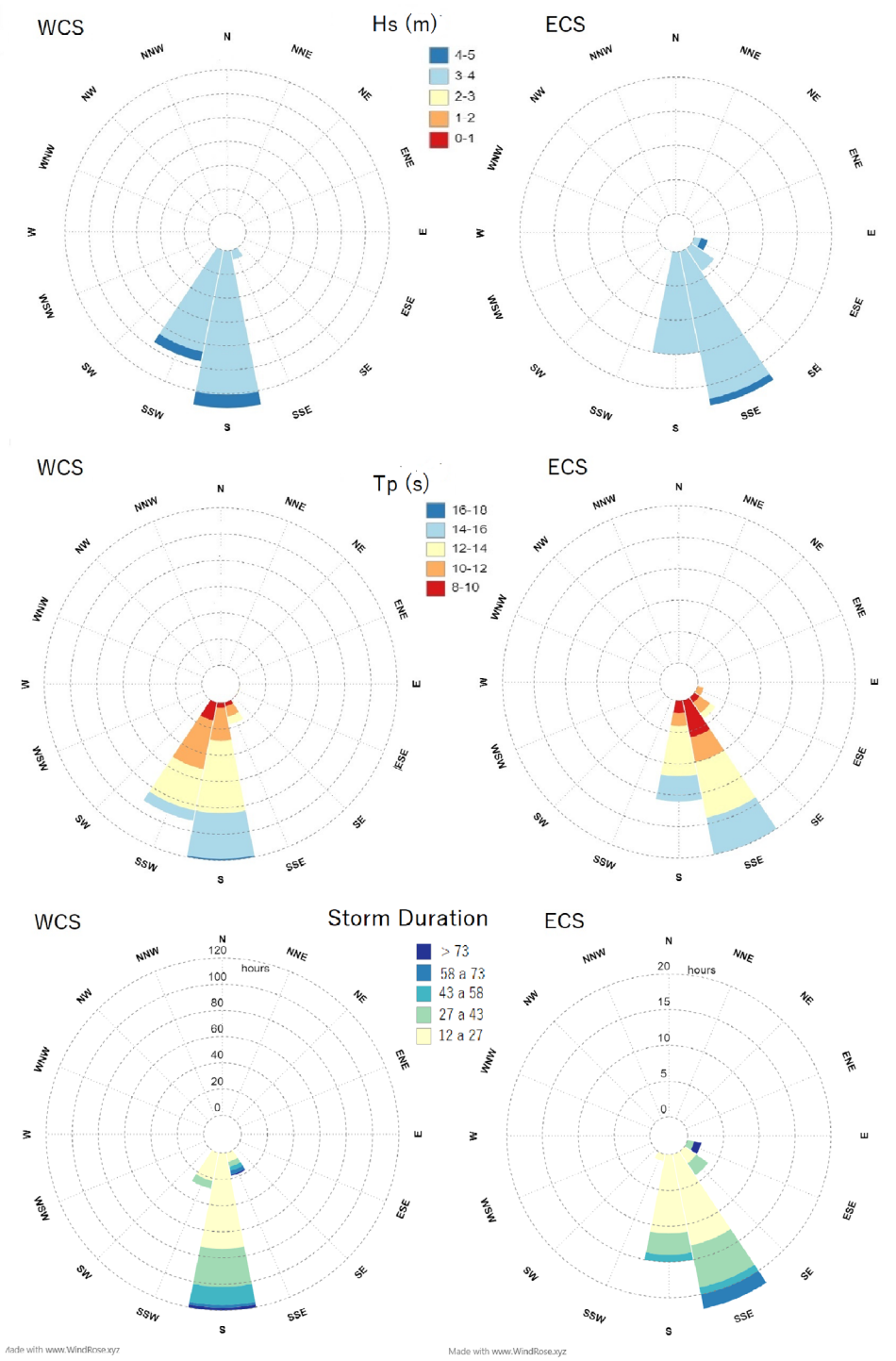

Figure 2. Wave roses represent Hs, Tp, and storm duration at WCS and ECS. Storm duration is given in hours.

Applying the Dolan and Davis (1992) SPI and the clustering method, the distribution of storms in Classes showed a log-normal pattern for both grid points (Figure 3). According to the methodology, five Classes of storms were identified within the respective range, as shown in Table 2. The analysis showed that the most frequent storm events occurred at the WCS for both Weak (Class I) and Moderate (Class II) classes. Extreme storms represented 3.4 % of occurrences. No Weak storms were identified at the ECS, with Moderate and Significant (Class III) storms being the most frequent, representing 31.8 % of occurrences. Severe (Class IV) and Extreme (Class V) storms represented 27 and 9 % of the occurrences at the ECS, respectively (Table 3).

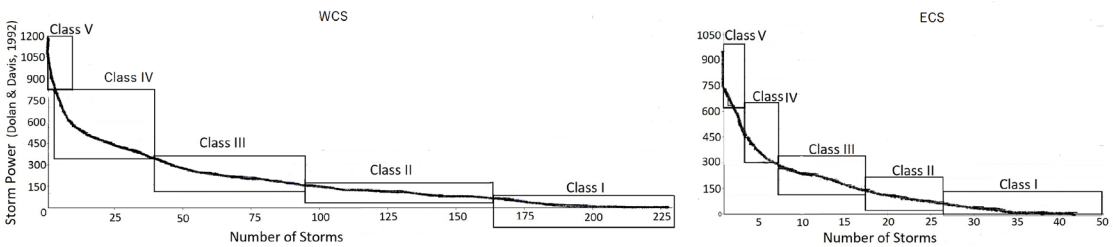

Figure 3. Storm classes obtained for WCS and ECS using Jenks' (1967) Natural Breaks function.

Table 2. Storm Power Index (SPI) classes and magnitude range of WCS and ECS

Storm Class		WCS SPI Range ($m^2\ h^{-1}$)	ECS SPI Range ($m^2\ h^{-1}$)
I	Weak	111 -197	5 - 75
II	Moderate	198 - 310	76 - 152
III	Significant	311 - 484	153 -300
IV	Severe	485 - 741	301 - 610
V	Extreme	742 - 1244	611 - 1059

Table 3. Characteristics of the five storm classes applying the Dolan and Davis methodology for WCS and ECS.

Storm Class	% of each Class		Hs (m)		Tp (s)		Duration (h)	
	WCS	ECS	WCS	ECS	WCS	ECS	WCS	ECS
I Weak	30	0	3.0 to 3.5	3.0 to 3.5	8 to 16	9.4 to 16.5	12 to 18	12 to 21
II Moderate	3.,6	31.8	3.0 to 4.0	3.1 to 3.5	9 to 16	8.7 to 15.1	18 to 30	18 to 27
III Significant	21.6	31.8	3.0 to 4.0	3.2 to 3.7	10 to 16	10 to 14	27 to 45	30 to 39
IV Severe	12.9	27.2	3.3 to 4.7	3.5 to 4.1	10 to 15	10 to 13	36 to 66	39 to 60
V Extreme	3.4	9	3.5 to 4.8	3.9 to 4.0	12 to17	10 to 12	54 to 90	66 to 90

At the WCS, storms of all classes came from the south and south-southeast directions but the latter occurred with lower frequency. Extreme storms from the south-southwest direction were absent. In contrast, at the ECS, only the south-southeast direction showed storms of all classes. Extreme storms emerged from the east-southeast direction but no such storms were observed from the south and southeast directions. The high frequency of storms from the south is common between the two locations. However, the frequency of south-southeast events shows a noticeable difference, which is significantly higher in ECS. Furthermore, no storm was observed from the south-southwest at ECS (Figure 4).

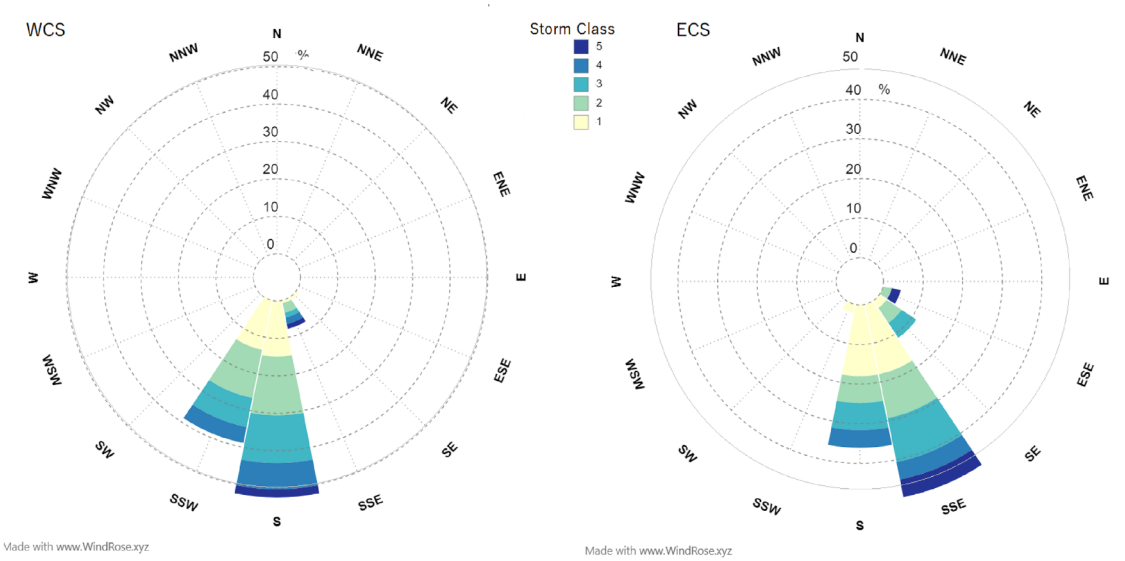

Figure 4. The wave rose represents the storm classes and their corresponding direction. The values are in percentages.

In total, 12 storms were classified as Extreme, with 8 identified at WCS and 4 at ECS. The characteristics of these storms are shown in Table 4. Among these, the most intense storm was the one that occurred in May 1997 at WCS, with a Storm Power of 1244 $m^2 h^{-1}$. The maximum wave height was recorded in July 2006, 4.7 m, whereas the longest storm lasted for 90 hours in September 1983 at ECS and August 2011 at WCS (as shown in Table 4). Regarding month distribution, Weak and Moderate storms were observed in the WCS every month of the year, whereas Significant and Severe storms occurred from March to November. Extreme storms were observed from April to September. Conversely, the ECS had an irregular distribution of storm events. No storm events occurred in January and February, whereas September showed all classes of events except class Weak. Extreme storms occurred in April, May, and September (Figure 5).

Table 4. Characteristics of the 12 Extreme storms (Class V) identified in the studied coastal sectors

Start Date	End Date	Grid Point	Mean Hs	Max Hs	Mean Tp	Mean Dp	SPI	Duration
Sep 25,1983	Sep 29, 1983	ECS	3.4	4.1	10	105	1059	90
Aug 8, 1988	Aug 13, 1988	WCS	3.8	4.5	12.8	172	1035	69
July 22, 1996	July 24, 1996	WCS	3.9	4.7	12,9	190	839	54
May 30, 1997	Jun 02, 1997	WCS	3.8	4.4	12	162	1244	84
May 31,1997	Jun 02, 1997	ECS	3.5	3.9	12	152	852	66
Sep 23, 1999	Sep 26, 1999	WCS	3.6	4.1	12	156	880	66
Sep 24, 1999	Sep 26, 1999	ECS	3.4	3.8	12	150	714	60
May 05, 2001	May 08, 2001	WCS	3.2	4.1	11	191	929	75
Jun 28, 2006	Jun 30, 2006	WCS	3.8	4.3	12.6	184	799	54
April 08, 2010	April 10, 2010	WCS	3.9	4.8	11.8	155	1142	72
April 08, 2010	April 10, 2010	ECS	3.6	4.1	12.3	151	756	57
Aug 21, 2011	Aug 25, 2011	WCS	3.3	3.5	14	186	996	90

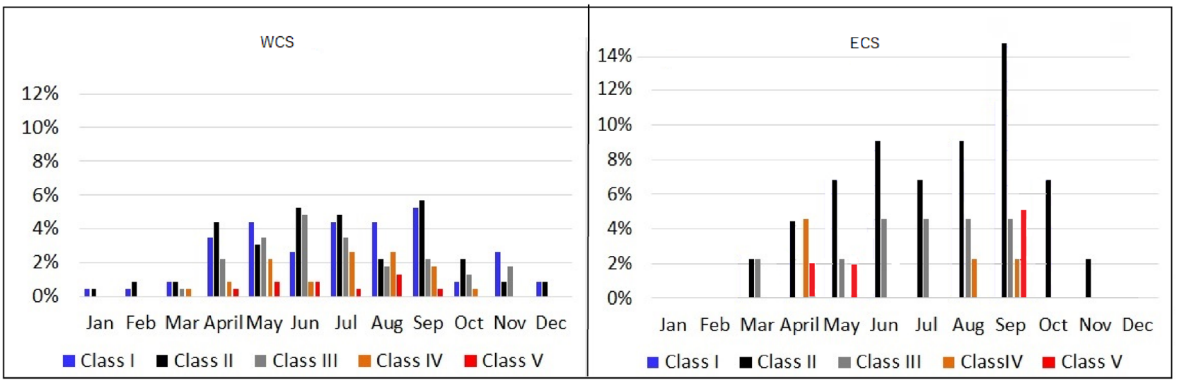

Figure 5. Monthly distribution of storms by Class regarding WCS and ECS areas.

Figure 6 displays the historical record of the maximum annual value of Storm Power and their relative moving averages. The time series analysis shows no statistically significant trends but an approximately cyclical behavior. The moving average illustrates similar troughs for both grid points in 1987, 1991-1994, 2000-2005, and 2008. Conversely, crests occurred in 1983, 1988-1990, 1995-1999, 2006-2007, and 2009-2012. The highest average annual Storm Power occurred at WCS in 1997 (848 m^2 h^{-1}), followed by 2011 (824 m^2 h^{-1}).

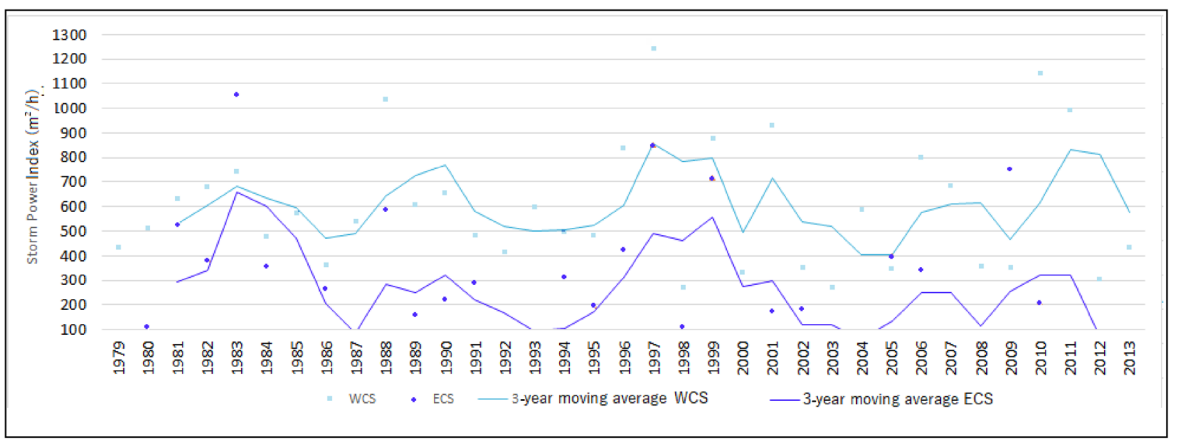

Figure 6. Time series of the annual maximum Storm Power and the 3-year moving average for WCS and ECS.

Regarding the return time of the maximum annual storm power, values below 550 m^2 h^{-1} correspond to storms between the classes Weak and Severe, with a return time of one year, indicating an annual probability of occurrence. For values up to 760 m^2 h^{-1}, which are associated with the class Severe, the return period is five years. The most significant return period is associated with the values of the May 1997 event. The storm class Extreme with the shortest return period, seven years, occurred in June 1996 (839 m^2 h^{-1}). Regarding the ECS point, storms of the class Moderate have a return period of one year. Extreme events have return periods between 23 (Sep 1999) and 100 years (Sep 1983) (Figure 7).

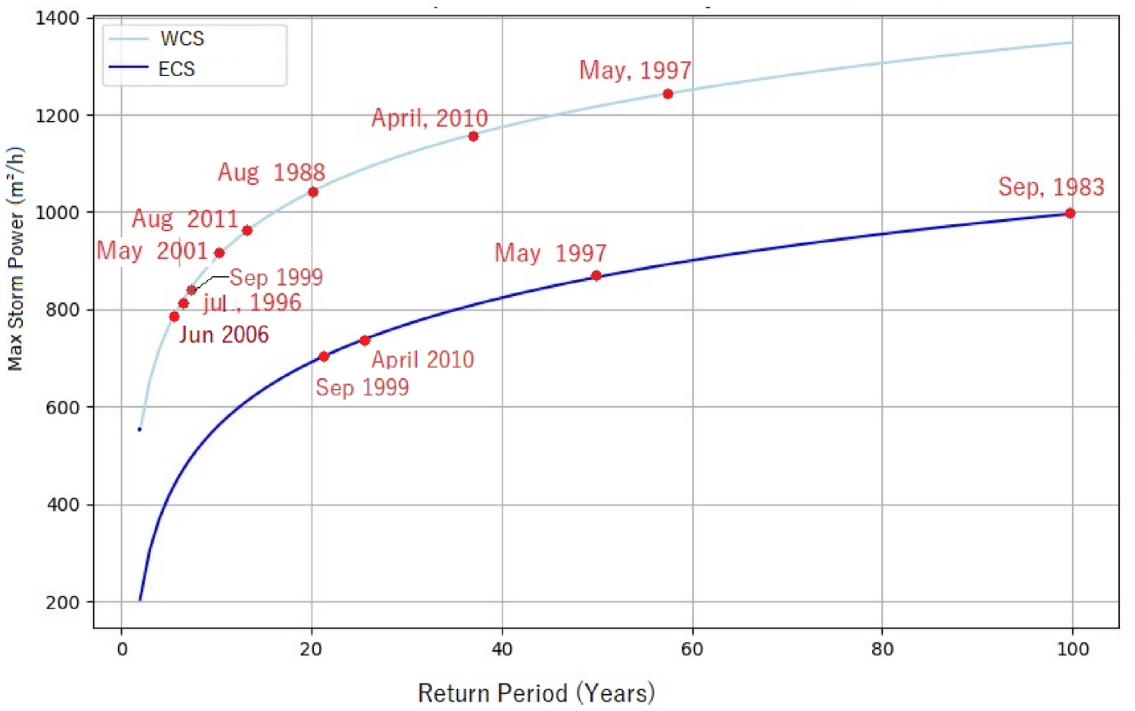

Figure 7. The storm returning period regarding the different storm classes at WCS and ECS. Red dots show the position of the greatest values of Extreme storms.

Wave propagation

According to the predominant direction of the storm, four events were chosen to be propagated to shallow waters, as shown in Table 5: the different impacts of the storm waves caused by the headlands of Cabo Frio and Cabo Búzios can be seen on a regional level, as shown in Figure 8. During the storms of 2001 (S) and 2007 (SSW), the wave energy failed to significantly decrease as it reached the WCS, whereas, in the ECS, energy attenuation was considerably more significant. A strong wave energy gradient was observed at the Cabo Frio embayment. In the 1983 (ESE) event, the Western sector experienced a more significant shadowing effect. The wave energy attenuation totaled about 50% during this event when compared to its initial conditions. The 2010 (SSE) event showed similarities between the two sectors, except for the more significant attenuation at the Cabo Frio embayment (Figure 8).

Table 5. Characteristics of the 4 storm events chosen as initial scenarios for wave propagation. The scenarios were propagated simultaneously at the same regional mesh, covering both coastal sectors.

Date	Hs (m)	Tp (s)	Dp (°)	Direction
September 1983	3.4	10	105	ESE
May 2001	3.2	11	191	S
May 2007	3.5	10	205	SSW
April 2010	3.9	11.8	151	SSE

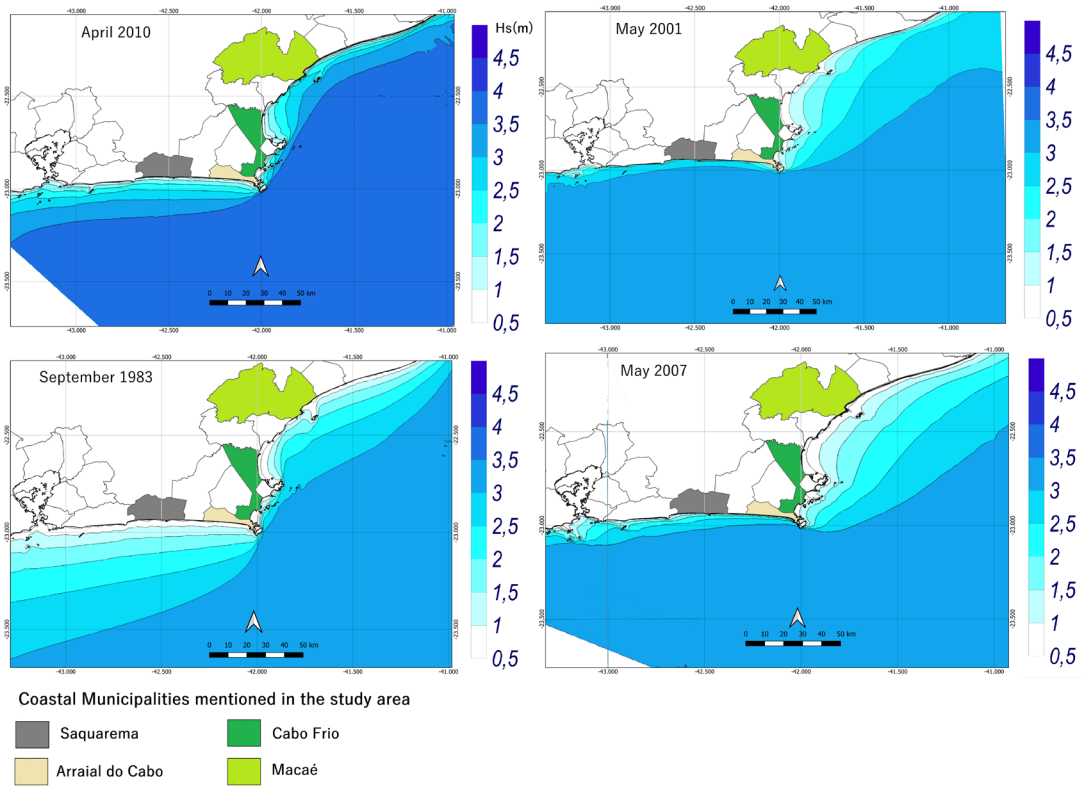

Figure 8. Propagated scenarios of storm waves according to Table 5.

Coastal Impact

Figure 9 summarizes the relation between storm classes and coastal impact. This study has found that the best correlation between storm classes and coastal impacts on the coast of Rio de Janeiro occurred in the Class Extreme for both WCS and ECS, resulting in severe beach and dune erosion, overwash, and property damage. Severe beach and dune erosion were also recorded as related to events classified as Severe, which also agrees with other authors. This study also found good agreement for the Weak Class. However, dune erosion was observed in WCS for the Weak and Moderate classes, a prediction absent from Dolan and Davis (1992).

Storm Class	Beach erosion			Dune erosion	Property damage	Overwash	References
	Weak	Moderate	Severe				
I	x●			●			Muehe, 2011;
II		x		●			Muehe, 2011.
III	x	x					Bulhões et al., 2016;
IV			●	●			Muehe, 2011; Lins-de-Barros et al., 2018
V	x	● x	● x	●x	●x	● x	Lins-de-Barros, 2005; Muehe, 2011; Fernandez et al., 2011; Lins-de-Barros et al., 2018; Carvalho et al., 2020

Figure 9. The relation between storm classes and coastal impact observed at WCS and ECS.

DISCUSSION

Storm Climatology

The storm climatology in this study is consistent with previous research conducted on the coast of Rio de Janeiro, which utilized the NCEP/WW3 hindcast database. These studies include Bulhões et al. (2010), Fernandez et al. (2011), Klumb-Oliveira et al. (2015), Muehe et al. (2015), Souza et al. (2015), Amorim and Bulhões (2016), Bulhões et al. (2016), Lins-de-Barros et al. (2018), and Carvalho et al. (2020). The findings of this study are also coherent with data collected *in situ* and those from regional and local runs of numerical models based on wind forcing (Rocha et al., 2004). Analysis indicates that higher energy waves are more frequent and stronger from April to September, coming predominantly from the south-southwest, south, and south-southeast, with wave heights up to 5 m. This study also found high wave heights from the eastern quadrants (east-southeast), which will be discussed later.

Regarding the number of storm events, Gramicianov et al. (2020) reported 87 high-energy wave events related to extratropical cyclones between 1999 and 2004 in the western portion of the South Atlantic, finding a similar average number of events per year (6.5) when compared to those in this study for the WCS, that is, 6.8 events per year. On the coast of Rio de Janeiro, Bulhões et al. (2014) found an average of 6.8 events per year (2003-2014) and Carvalho et al. (2020), an average of 5.1 events per year (1986 – 2018).

Regarding the relation between cyclogenesis and coastal storms, Gan and Rao (1991) found 1091 cyclones over South America (15°-50°S to 30°-90°W) from 1979 to 1988, whereas Reboita et al. (2010), 2760 cyclogenesis over the Southern Atlantic Ocean (5°-60°S to 84°W-15°E) from 1990 to 1999.

During the same period as Reboita et al. (2010) (1990-1999), 66 storm events were identified on the coast of Rio de Janeiro at the WCS, of which three were classified as Extreme. On the other hand, 16 storm events were identified at the ECS, of which two were classified as Extreme (as shown in Table 4). These numbers represent 2.39 and 0.57% of all cyclones in the literature. In general, it seems that only a small number of cyclones in the western South Atlantic have caused coastal storms in the study locations. However, this conclusion may be limited by the methodology used to identify storms (only those with waves higher than 3 m and lasting at least 12 hours were considered). It is possible that storms with lower wave heights (as low as 1.8 m, as suggested by Lins-de-Barros et al., 2018) may still have damaged or eroded the coast. Also, it should be noted that the NCEP/WW3 hindcast may have limitations in its spatial resolution and wind forcing, which could result in weaker Hs values, although an overestimation of the model has been found when compared to a stationary buoy near the study area. However, a research study conducted by Lins-de-Barros et al. (2018) found 120 days of high-energy sea states on newspapers regarding the beaches in the state of Rio de Janeiro from 1979 to 2013. This and the aforementioned studies support previous observations that the number of coastal storms is low compared to the total number of cyclone events in the literature. Further analysis can be conducted to more accurately evaluate the impact of cyclone trajectory and speed along the South Atlantic, which could damage the coast of Rio de Janeiro. For instance, Gramicianov et al. (2020) noted a correlation between the speed of cyclone displacement and the duration and formation of high-energy waves. A slower displacement increases the likelihood of extreme wave generation.

The results of this study show that the duration of storm events is similar to that reported by Carvalho et al. (2020), which was around 27 hours. However, it differs from the observations made by Bulhões et al. (2014) and Souza et al. (2015) on the Campos Basin coast, in which the duration of storm events lasted approximately 36 hours. Apart from the differences in shelf morphology and coastal orientation between the Campos and Santos Basins, the influence of SASH in the storm duration is remarkable. It is worth noting that the ECS has shown storm events lasting over 70 hours, which originated from the east-southeast direction. An event that lasted 90 hours, from September 25 to 29, 1983, had a maximum wave height of 4 meters and a mean direction of 108°. Amorim

and Bulhões (2015) found similar storm behavior in the storm event on November 23, 2008, with a wave height of up to 3.2 m and stemming from the east-southeast. These characteristics may be linked to the interaction between extratropical cyclones and SASH, as discussed by Gramicianov et al. (2020). That article explains that SASH could obstruct the eastward movement of a cyclone, resulting in a limited trajectory and slower speed.

Although not the primary focus of this study, it is worth mentioning that the El Nino Southern Oscillation (ENSO) can impact the wave climate around the oceans by changing wind patterns, pressure cells, and cyclone density (Reboita et al.,2015; Godoi et al., 2020). Some studies, such as Pereira and Klumb-Oliveira (2015) and Carvalho et al. (2020), have linked the wave climate of the Rio de Janeiro coast with the phases of ENSO. Pereira and Klumb-Oliveira (2015) found that years of negative ENSO (La Nina) showed a gradual increase in wave height, whereas, in years of positive ENSO (El Nino), the wave height decreased, with a four-month lag response. Carvalho et al. (2020) found a slightly higher frequency of storms during years of El Nino.

In this study, if considering the four-month lag response — as per Pereira and Klumb-Oliveira (2015) —, among the identified Extreme storm events, it was observed that those in 1983 and 1997 occurred during a positive ENSO phase, whereas those in 1988, 1999, and 2006, during a negative phase. It was also observed that the average Hs of the Extreme storms during El Nino were slightly lower than those during La Nina, as mentioned by the authors. Also, the frequency of extreme storm events was found to be higher during La Nina than El Nino.

It is also important to mention that many other climate variability modes, including a complex suit of teleconnections alongside ENSO, could affect wave climate and coastal storms. For instance, the Southern Annular Mode is expected to influence the trajectory and density of cyclones in the South Atlantic and, thus, storm waves. Reboita et al. (2015) found that the positive (negative) phase of the Southern Annular Mode leads to a higher (lower) density of cyclones in South Atlantic sub-latitudes. This can directly affect the storm wave patterns and behavior on the South and Southeast Brazil coast. In this study, the negative phase of the Southern Annular Mode occurred during the Extreme storms in September 1983 and May 1997, whereas those in 1988, 1999, and 2011 occurred during its positive phase. However, further examination is necessary to best correlate the ocean-atmosphere mode to coastal storms in Rio de Janeiro.

Storm Classification

The range values of the storm classes in this study significantly differed from those initially found by Dolan and Davis (1992) for the north easterlies extratropical cyclones of the North Atlantic, which mainly concerned the Severe and Extreme classes and showed values > 2322.5 $m^2 h^{-1}$ and > 929, respectively. This is related to the higher Hs values (>7 m) and duration (>96 h) found by those authors in the North Atlantic than those found in this study. Rangel-Buitrago and Anfuso (2011) applied the Dolan and Davis (1992) methodology to the Atlantic side of the Andalusia Region (Spain). The authors found even higher values for Storm Power, such as > 4669 $m^2 h^{-1}$ for the Extreme and > 2341 for the Severe Classes, also due to Hs values above 6.6 m and storm durations above 150 h.

After comparing the range of Storm Power obtained for the West Coast of the state of Rio de Janeiro by Carvalho et al. (2020) with the findings of this study, similar values were observed for all classes. However, the values obtained by the authors were more significant for the Extreme class. These differences are probably due to different clustering methods and possible local variations in wave field and shelf topography at the chosen grid point. However, the events of May 2001 and April 2010 were identified in both works as Extreme Class, which shows the ability of the method to identify the most intense storm episodes, even considering different grouping techniques or local differences. Those Extreme storm events were also found in Lins-de-Barros (2005), Fernandez et al. (2011), and Muehe et al. (2015) for the coast of Rio de Janeiro and in Rudorff et al. (2014) for the coast of Santa Catarina. Additionally, the cyclogenetic activity associated with the Extreme

coastal storms in August 1988, May 2001, and August 2011 (Table 4) are also featured in the literature as in Innocentini and Caetano Neto (1996), Innocentini and Prado (2003), and Abreu et al. (2018), respectively.

Concerning return periods, the results in this study are consistent with those in Carvalho et al. (2020) regarding the Weak to Significant Classes but differ from those for the Extreme class for May 2001 and April 2010. This could lead to further analyses seeking patterns of return by comparing methodologies. The differences between analyzed grid points may represent different wave energy patterns along the coast and a longitudinal gradient of wave energy. This is because the Storm Power value obtained by the authors above for the May 2011 event totaled 1522 $m^2 h^{-1}$, whereas the value in this study, totaled only 929 $m^2 h^{-1}$. The difference in values is due to the duration of the event, which lasted for 93 hours when compared to the 75 hours in this study.

Storm Propagation and Coastal Impact

The effect of wave refraction and shadow zones in controlling storm erosion on coastal headlands is featured in the literature (Hsu and Evans,1989). Fellowes et al. (2022) noted a 3.5 times greater loss of beach volume on exposed than shaded beaches on the east coast of Australia. At the coastline of Rio de Janeiro, according to Muehe (2011), the retreat of the crest of the foredune of Massambaba Beach, in the Western sector, was approximately 50 % greater in the Extreme storm of May 2001 (190°) than the 2010 (160°) storm event and significantly greater than May 1997 (168°) event. Aside from the fact that sedimentary and morphodynamical aspects and morphodynamical beach states prior to the storm strongly control the local impact on the coastline, the differences between the retreat of the foredune draw attention to the attenuation effect of the WCS to the storms coming from the eastern octants. A similar shadowing effect was observed by Souza et al. (2015) on the north coast of the state of Rio de Janeiro, in which different levels of coastal storm exposure were found due to a change in the orientation of the coastline in Cape São Tomé.

An aspect that affects the dissipation of waves is the difference in morphology between the WCS and the (ECS). The ECS has a smoother and gentler slope, which causes most of its wave energy to dissipate at its shoreface. This observation was made by Guimarães et al. (2014), who noticed that the south of Patos lagoon, in Rio Grande do Sul State, had greater wave energy dissipation due to the smoother slope of its shoreface.

Another issue concerns the average depth of the grid points in this study. Gramicianov et al. (2020), using the NCEP/WW3 hindcast, point out that the depth to be considered as deep water for wave climate analysis should be deeper than 610 m. Thus, the average depths of the grid points in this work already represent shallow water and, therefore, reflect the effects of bottom dissipation and refraction. On the other hand, Camus et al. (2011) highlight that the physics of waves in shallow waters, e.g., refraction, diffraction, energy dissipation, and white-capping, are generally excluded from global hindcast/reanalysis data because, even if the physics of the computational model considers such processes, the grid associated with Global resolution bathymetry makes it challenging to process them in shallow areas, which leads to the need for downscaling to better understand the wave climate in coastal areas. Thus, the hindcast resolution is a limitation that affects this and the previous study in the region. Future research could apply better resolution hindcasts, which are already available, such as the Global Ocean Waves Reanalysis (Law-Chune et al., 2021).

The correlation between storm classes and their impacts on the coast is complex given the multifactorial nature of the coastal process. The orientation of the coast, its morphodynamical stage, its frequency of storm events, and the regional and local characteristics of the inner shelf are aspects that act together to attenuate or amplify storm events. In any case, the events identified in this study as Extreme resulted in impacts similar to those predicted in the model proposed by Dolan and Davis, such as beach and dune erosion, overwash, and property damage. Conversely, foredune crest retreat occurred in storms classified as Weak and Moderate. This

reinforces the importance of other factors related to the vulnerability of the coast to storm impacts, including the method sensitivity to the minimum threshold of Hs and td.

CONCLUSION

This study aimed to identify, classify, and evaluate the impacts of storm events based on an easy-to-apply methodology. The SPI index is susceptible to the two chosen variables (Sh, td) and the defined storm thresholds. Furthermore, it fails to encompass the surge (the sea level oscillations responsible for wave set-up) and, thus, potential coastal inundation. However, the wave energy is considered when evaluating the square of the maximum wave height. Thus, even the small differences between wave heights can represent more significant differences in Storm Power, which is pertinent regarding local variation assessments. Still, it is featured in the literature that the longer the storm, the greater the coastal impact, which makes it a valuable methodology for coastal vulnerability applications.

Classifying storms into five classes proved a suitable methodology since it managed to hierarchize and characterize each class, infer their return times, and estimate the coastal risks associated with each class. It is possible that storm events that significantly damaged the coast had an Sh lower than 3 m, but these are absent from this study. As discussed earlier, future research could apply this methodology to update storm data to the present day using higher hindcast resolution data. Finally, the west and east coasts show heterogeneous coastal geomorphology and shelf geomorphic characteristics. Thus, the coastal response will be different on each particular coastal side. In any case, coastal orientation has remarkably influenced coastal protection.

ACKNOWLEDGMENTS

The author would like to express his gratitude to the reviewers of the Ocean and Coastal Research Journal for their valuable contributions to this study.

AUTHORS CONTRIBUTIONS

L.K: Conceptualization; Investigation; Methodology; Formal analisys; Data curation; Software; Writing - original draft preparation; Writing - review and editing.

REFERENCES

Abreu, E. X., Silva, M. V., Reboita, M. S. & Teodoro, T. A. 2018. Estudo do ciclo de vida de três ciclones extratropicais no Oceano Atlântico Sul (Life cycle study of three extratropical cyclones in the South Atlantic). *Revista Brasileira de Geografia Física*, 11(1), 251–275.

Amorim, I. B. S & Bulhões, E. M. R. 2016. Análise das condições sinóticas de eventos de ondas de tempestade no litoral norte Fluminense. *Boletim do Observatório Ambiental Alberto Ribeiro Lamego*, 10(1), 253-279. DOI: https://doi.org/10.19180/2177-4560.v10n12016p253-279

Allen, J. R. 1981. Beach erosion as a function of variations in the sediment budget. Sandy Hook, New Jersey, USA. *Earth Surface and Landforms*, 6(2), 139–150. DOI: https://doi.org/10.1002/esp.3290060207

Barletta, R. C. & Calliari, L. J. 2002. Determinação da Intensidade das Tempestades que atuam no litoral do Rio Grande do Sul, Brasil. *Pesquisas em Geociências*, 28(2), 117–124. DOI: https://doi.org/10.22456/1807-9806.20276

Battjes, J. & Groenendijk, H. 2000. Wave height distributions on shallow foreshores. Coastal Engineering, 40(3), 161-182. DOI: https://doi.org/10.1016/S0378-3839(00)00007-7

Bruun, P. M. 1962. Sea Level rise as a cause of shore erosion. *Journal of the Waterways and Harbors Division*, 88, 117130

Bulhões, E. M., Fernandez, G. B. & Rocha, T. B. 2010. Efeitos morfológicos nas barreiras costeiras do litoral centro-norte do estado do Rio de Janeiro: resultados do evento de tempestade de abril de 2010. *Revista de Geografia*, (2), 15–29.

Bulhões, E., Fernandez, G. B. Oliveira Filho, S. R., Pereira, T.G. & Rocha, T.B. 2014. Impactos Costeiros Induzidos por Ondas de Tempestade entre o Cabo Frio e o Cabo Búzios, Rio de Janeiro, Brasil. *Quaternary and Environmental Geosciences*, 5(2), 155–165.

Bulhões, E., Fernandez, G. B., Oliveira Filho, S. & Pereira, T. G. 2016. Coastal Impacts Induced by Storm Waves between Cape Frio and Cape Buzios, Rio de Janeiro, Brazil. *Journal of Coastal Research*, 75(sp1), 1047–1051.

Carvalho, B C., Dalbosco, A. L. P. & Guerra, J. V. 2020. Shoreline position change and the relationship to annual and interannual meteo-oceanographic conditions in Southeastern Brazil. *Estuarine, Coastal and Shelf Science*, 235, 106582. DOI: https://doi.org/10.1016/j.ecss.2020.106582

Campos, R. M., Alves, J.-H. & Parente, C. E. 2013. Modelagem de Ondas Extremas no Oceano Atlântico Sul. In: X Simpósio sobre Ondas, Marés, Engenharia Oceânica e Oceanógrafa por Satélite OMAR-SAT (10th. ed.).

Camus, P., Mendez, F. J. & Medina, R. 2011. A hybrid efficient method to downscale wave climate to coastal areas. *Coastal Engineering*, 58(9), 851–862. DOI: https://doi.org/10.1016/j.coastaleng.2011.05.007

Collins, J. I. 1970. Probabilities of Breaking Wave Characteristics. *Coastal Engineering*, 12 DOI: https://doi.org/10.9753/icce.v12.25

Dolan, R. & Hayden, B. 1983. Patterns and Prediction of Shoreline Change. *In*: Komar, P. D. & Moore, J. R.

Handbook of coastal process and erosion (pp. 123-150). Boca Raton, CRC Press.

Dolan, R. & Davis, R. E. 1992. An intensity scale for Atlantic coast northeast storms. *Journal of Coastal Research*, 8(3), 840–853.

Durán, R., Guillén, J., Ruiz, A., Jiménez, J. A. & Sagristà, E. 2016. Morphological changes, beach inundation and overwash caused by an extreme storm on a low-lying embayed beach bounded by a dune system (NW Mediterranean). *Geomorphology*, 274, 129–142. DOI: https://doi.org/10.1016/j.geomorph.2016.09.012

Earlie, C., Masselink, G. & Russell, P. 2018. The role of beach morphology on coastal cliff erosion under extreme waves. *Earth Surface Processes and Landforms*, 43(6), 1213–1228. DOI: https://doi.org/10.1002/esp.4308

Fernandez, G. B., Bulhões, E. & Rocha, T. B. 2011. Impacts of Severe Storm Occurred in April 2010 along Rio de Janeiro Coast, Brazil. *Journal of Coastal Research*, 1850–1854.

Fellowes, T., Vila-Concejo, A., Gallop, S., Harley, M. D. & Short, A. 2022. Wave shadow zones as a primary control of storm erosion and recovery on embayed beaches. *Geomorphology*, 399, 108072. DOI: https://doi.org/10.1016/j.geomorph.2021.108072.

Figueiredo Jr, A. G. & Tessler, M. 2004. *Topografia e composição do substrato marinho da região Sudeste-Sul do Brasil*. São Paulo: Instituto Oceanográfico.

Figueiredo Jr, A. G., Pacheco, C. E. P., Vasconcelos, S. C. & Silva, F. T. 2016. Continental shelf geomorphology and sedimentology. *In*: Kowsmann, R. O. *Geology and Geomorphology* (pp. 13-31). Amsterdam: Elsevier. DOI: https://doi.org/10.1016/b978-85-352-8444-7.50009-3.

Figueiredo Jr, A., Carneiro, J. C., & Santos Filho, J. R. D. 2023. Santos Basin continental shelf morphology, sedimentology, and slope sediment distribution. *Ocean and Coastal Research*, 71(Suppl. 3). DOI: https://doi.org/10.1590/2675-2824071.22064agfj.

Gan, M. A. & Rao, V. B. 1991. Surface cyclogenesis over South America. *Monthly Weather Review*, 119(5), 1293–1303. DOI: https://doi.org/10.1175/1520-0493(1991)119<1293:SCOSA>2.0.CO;2

Godoi, V. A, Andrade, F., Durrant, T. H. & Torres Jr, A. 2020. What happens to the ocean surface gravity waves when ENSO and MJO phases combine during the extended boreal winter? *Climate Dynamics*, 54(3–4), 1407–1424. DOI: https://doi.org/10.1007/s00382-019-05065-9.

Guimarães, P. V., Farina, L. & Toldo Jr, E. E. 2014. Analysis of extreme wave events on the southern coast of Brazil. *Natural Hazards and Earth System Sciences*, 14(12), 3195–3205.

Gramcianinov, C. B., Campos, R. M., Guedes, C. & Camargo, R. 2020. Extreme waves generated by cyclonic winds in the western portion of the South Atlantic Ocean. *Ocean Engineering*, 213, 107745. DOI: https://doi.org/10.1016/j.oceaneng.2020.107745

Harley, M. 2017. Coastal Storm Definition. *In*: Ciavola, P. & Coco, G. *Coastal Storms: Processes and Impacts*. Hoboken: John Wiley and Sons.

Hsu, J.R.C. & Evans, C. 1989. Parabolic Bay Shapes and Applications. Proceedings, institution of civil engineers, 87(2), 557–570.

Innocentini, F. A. O. & Prado, S. C. 2003. Modelo de ondas aplicado ao caso 5-8 de maio de 2001. *Revista Brasileira de Meteorologia*, 18(1), 97–104.

Innocentini, V. E. & Caetano Neto, S. 1996. A Case Study of the 9 August 1988 South Atlantic Storm: Numerical simulations of the Wave Activity. *Weather and Forecasting*, 11(1), 78–88.

Jenks, G. F. 1967. The Data Model Concept in Statistical Mapping. *International Yearbook of Cartography*, 7, 186–190.

Klumb-Oliveira, L. A., Pereira, N. E. S. & Leão, R. R. 2015. Multitemporal morphodynamics in reflective beach in central and Northern coast of RJ in response to regional wave climate. *Revista Brasileira de Geomorfologia*, 16(1), 19–36.

Kutupoglu, V., Çalişir, E. & Akpinar', A. 2023. Characterization and classification of wave storm events and wave climate on the Sea of Marmara. *Ocean Engineering*, 279, 114448. DOI: https://doi.org/10.1016/j.oceaneng.2023.114448

Law-Chune, S., Aouf, L., Dalphinet, A., Levier, B., Drillet, Y. & Drevillon, M. 2021. WAVERYS: a CMEMS global wave reanalysis during the altimetry period. *Ocean Dynamics*, 71, 357–378. DOI: https://doi.org/10.1007/s10236-020-01433-w

Lins-de-Barros, F. M., Klumb-Oliveira, L. A & Lima, R. 2018. Avaliação histórica da ocorrência de ressacas marinhas e danos associados entre os anos de 1979 e 2013 no litoral do estado do Rio de Janeiro (Brasil). Revista de Gestão Costeira Integrada, 18(2), 85–102. DOI: https://doi.org/10.5894/rgci-n146

Lins-de-Barros, F. M. 2005. Risco, Vulnerabilidade Física à Erosão Costeira e Impactos Socioeconômicos na Orla Urbanizada do Município de Maricá, Rio de Janeiro. *Revista Brasileira de Geomorfologia*, 6(2), 83–90. DOI: https://doi.org/10.20502/rbg.v6i2.54

Mitchell, J. K. 1974. *Community Response to Coastal Erosion: Individual and Collective adjustments to Hazard on the Atlantic Shore*. Chicago, The University of Chicago.

Muehe, D. & Valentini, E. 1998. *O Litoral do Estado do Rio de Janeiro: uma caracterização físico-ambiental.* Rio de Janeiro, FEMAR.

Muehe, D. 2011. Erosão costeira - Tendência ou eventos extremos? O litoral entre Rio de Janeiro e Cabo Frio, Brasil. *Revista da Gestão Costeira Integrada*, 11(3), 315–325.

Muehe, D., Lins-de-Barros, F., Oliveira, J. & Klumb-Oliveira, L. A. 2015. Pulsos erosivos e resposta morfodinâmica associada a eventos extremos na costa leste do estado do Rio de Janeiro. *Revista Brasileira de Geomorfologia*, 16(3). DOI: https://doi.org/10.20502/rbg.v16i3.728

Naiqiang, L. & Guiyang, X. 2020. Grid analysis of land use based on natural breaks (Jenks) classification. *Bulletin of Surveying and Mapping*, (4), 106–110.

Ojeda, E., Appendini, C. M. & Mendoza, E. T. 2017. Storm-wave trends in Mexican waters of the Gulf of Mexico

and Caribbean Sea. *Natural Hazards and Earth System Sciences*, 17(8), 1305–1317. DOI: https://doi.org/10.5194/nhess-17-1305-2017

Parente, C. E., Nogueira, I. C. M., Martins, R. P. & Ribeiro, E. O. 2016. Climatologia de Ondas. *In*: Martins, R. P., Grossmann-Matheson, G. S., Falcão, A. P. & Curbelo-Fernandez, M. P. (eds.). *Caracterização Ambiental Regional da Bacia de Campos, Atlântico Sudoeste: Meteorologia e Oceanografia* (pp. 55-98). Rio de Janeiro: Elsevier.

Parise, C. K., Calliari, L. J. & Krusche, N. 2009. Extreme storm surges in the South of Brazil: Atmospheric conditions and shore erosion. *Brazilian Journal of Oceanography*, 57(3), 175–188.

Paula, D. P., Morais, J. O., Ferreira, Ó. & Dias, J. A. 2015. Análise histórica das ressacas do mar no litoral de Fortaleza (Ceará, Brasil): origem, características e impactos. *In*: Paula, D. P. & Dias, J. A. (orgs.). *Ressacas do Mar, Temporais e Gestão Costeira* (pp. 173-201). Fortaleza: Premius.

Poli, P. 2011. Data Assimilation for Atmospheric Reanalysis. *In*: *Seminar on Data assimilation for atmosphere and ocean*.

Rangel-Buitrago N. & Anfuso, G. 2011. An application of Dolan and Davis (1992) classification to coastal storms in SW Spanish littoral. *Journal of Coastal Research*, 64, 1891–1895.

Reboita, M. S., Iwabe, C., da Rocha, R. P. & Ambrizzi, T. 2009. Análise de um ciclone semi-estacionário na Costa Sul do Brasil associado a bloqueio atmosférico. *Revista Brasileira de Meteorologia*, 24(4), 407–422.

Reboita, M. S, da Rocha, R. P., Ambrizzi, T. & Sugahara, S. 2010. South Atlantic Ocean Cyclogenesis Climatology Simulated by Regional Climate Model (RegCM3). *Climate Dynamics*, 35, 1331-1347.

Reboita, M. S., da Rocha, R. P., Ambrizzi, T. & Gouveia, C. D. 2015. Trend and teleconnection patterns in the climatology of extratropical cyclones over the Southern Hemisphere. *Climate Dynamics*, 45, 1929–1944.

Reis, A. T., Maia, R. M. C., Silva, C. G., Rabineau, M., Guerra, J. V., Gorini, C., Ayres, A., Arantes-Oliveira, R., Benabdellouahed, M., Simões, I. & Tardin, R. 2013. Origin of step-like and lobate seafloor features along the continental shelf off Rio de Janeiro State, Santos basin-Brazil. *Geomorphology*, 203, 25–45. DOI: http://dx.doi.org/10.1016/j.geomorph.2013.04.037.

Rocha, R. P., Sugahara, S. & Silveira, R. B. 2004. Sea Waves Generated by Extratropical Cyclones in the South Atlantic Ocean: Hindcast and Validation against Altimeter Data. *Weather and Forecasting*, 19(2), 398–410. DOI: https://doi.org/10.1175/1520-0434(2004)019<0398:SWGBEC>2.0.CO;2

Rudorff, F. M., Bonetti Filho, J., Moreno, D. A., Oliveira, C. A. F & Murara, P. G. 2014. Maré de tempestade. *In*: Herrmann, M. L. P. (org.). *Atlas de desastres naturais do Estado de Santa Catarina: período de 1980 a 2010*. 2nd. ed. Florianópolis: Cadernos Geográficos.

Saha, S., Moorthi, S., Pan H.-L., Wu, X., Wang, J., Hou, Y.-T., Juang, H.-M. H., Sela, J., Iredell, M., Treadon, R., Kleist, D., Van Delst, P., Keyser, D., Derber, J., Ek, M., Meng, J., Wei, H., Yang, R., Lord, S., van den Dool, H., Kumar, A., Wang, W., Long, C., Chelliah, M., Xue, Y., Huang, B., Schemm, J.-K., Ebisuzaki, W., Lin, R., Xie, P., Chen, M., Zhou, S., Higgins, W., Zou, C.-Z., Liu, Q., Chen, Y., Han, Y., Cucurull, L., Reynolds, R. W., Rutledge, G. & Goldberg, M. 2010. The NCEP climate forecast system reanalysis. *Bulletin of the American Meteorological Society*, 91(8), 1015-1058. DOI: https://doi.org/10.1175/2010BAMS3001.1

Shepard, F. P. 1950. *Longshore Bars and Longshore Troughs*. Washington, D.C.: Army Corps of Engineers.

SMC (Sistema de Modelagem Costeira). 2017. *Manual de Referência – Modelo de Propagação de Ondas Espectrais em Praias*. Brasília, DF: Ministério do Meio Ambiente.

Sondermann, M., Chou, S. C., Souza, C. R. G., Rodrigues, J. & Caprace, J. D. 2023. Atmospheric patterns favorable to storm surge events on the coast of São Paulo State, Brazil. *Natural Hazards*, 117(1), 93–111. DOI: http://dx.doi.org/10.1007/s11069-023-05851-z

Souza, T, A; Bulhões, E. & Amorim, I. B. S. 2015. Ondas de tempestade na costa Norte Fluminense. *Quaternary and Enviromental Geosiences*, 6(2),10-17. DOI: http://dx.doi.org/10.5380/abequa.v6i2.41139

Tolman, H. L. 2009. *User Manual and System Documentation of WAVEWATCHIII version 3.14*. Calm Springs: U. S. Department of Commerce. National Oceanic and Atmospheric Administration. National Weather Service. National Centers for Environmental Prediction. Technical Note.

You, Z. & Lord, D. 2008. Influence of the El Niño–Southern Oscillation on NSW Coastal Storm Severity. *Journal of Coastal Research*, 24(sp2), 203–207. DOI: https://doi.org/10.2112/06-0690.1

Zhang, K. Q., Douglas, B. C. & Leatherman, S. P. 2000. Twentieth century storm activity along the U.S. east coast. *Journal of Climate*, 13(10), 1748–1761. DOI: https://doi.org/10.1175/1520-0442(2000)013<1748:TCSAAT>2.0.CO;2